



Darcy-Benard surface tension driven convection in a composite layer with temperature dependent heat source

R. Sumithra¹, M. A. Archana^{2*} and R. K. Vanishree³

Abstract

The effect of temperature dependent heat source on single component Benard Surface tension driven convection in a composite layer system comprising of an incompressible fluid saturated porous layer underlying a layer of same fluid, is studied. The lower surface of the porous layer is rigid and the upper surface is free with surface tension depending on temperature. The governing partial differential equations are non-dimensionalized using suitable transformation variables. The eigen value problem obtained after normal mode analysis is solved analytically using Exact Method. An expression for the eigenvalue, the Thermal Marangoni number is obtained for two sets of thermal boundary conditions on the boundaries of the composite layer, set (i) Adiabatic-Adiabatic and set (ii) Isothermal-Adiabatic. The effects of different physical parameters on the same are discussed in detail.

Keywords

Composite layer, Surface tension driven convection, Temperature dependent heat source.

AMS Subject Classification

78Axx.

^{1,2} Department of UG, PG Studies and Research in Mathematics, Government Science College Autonomous, Bengaluru, Karnataka, India.

³ Department of Mathematics, Maharani Science College for Women, Maharani Cluster University, Bengaluru, Karnataka, India.

*Corresponding author: ¹sumitra.diya@yahoo.com; ²archanamurthy78@gmail.com; ³vanirkmscw@gmail.com;

Article History: Received 16 September 2020; Accepted 09 November 2020

©2020 MJM.

Contents

1	Introduction	2074
2	Formulation of the Problem	2075
3	Boundary Conditions	2076
4	Method of Solution	2076
4.1	Thermal Marangoni number for the set (i) Adiabatic - Adiabatic (A-A) condition	2077
4.2	Thermal Marangoni number for the set (i) Adiabatic -Isothermal (A-I) condition	2077
5	Result and Discussion	2078
6	Conclusion	2081
	References	2081

1. Introduction

Convection is the physical phenomenon that involves heat exchange through two systems. The interaction between a

saturated porous layer overlying a fluid layer and convection in such a configuration is encountered in many industrial and environmental applications such as extraction of oil from underground reservoirs, packed-bed thermal storage systems, solidification of alloys, the manufacturing of composite materials used in aircraft and etc. Surface tension driven convection or Marangoni convection is the tendency for heat and mass to travel to areas of higher surface tension within a fluid and has many industrial applications such as semiconductor processing, welding, heat exchangers crystal growth, effect around vapour bubbles during nucleation and also in the field of space technology. There are few works available on Marangoni convection in two layer systems. Nield [5] has investigated the linear stability problem of superposed fluid and porous layers with buoyancy and surface tension effects at the deformable free upper surface by using Beavers-Joseph slip condition at the interface. While Nield [6] also argued about the modelling of Marangoni convection in a fluid saturated porous medium and has suggested the consideration of composite system in analyzing the problem of fluid-porous layer. The

study of Marangoni convection has attracted many researchers in recent years because of its vast contributions in various industries. Shivakumara et al. [10] investigated the effect of internal heat generation on Marangoni convection in a fluid layer overlying a layer of anisotropic porous medium. The resulting eigen value problem is solved using regular perturbation technique. An expression for critical Marangoni number is obtained, possibilities of controlling Marangoni convection is discussed in detail. Gangadharaiah [3] studied the stability analysis of B ard-Marangoni convection in a composite system theoretically by using regular perturbation technique. The phenomenon of non-uniform heat source/sink has many engineering applications like cooling of metallic sheets, the intention of thurst bearing, unpolished oil retrieval, etc. Theoretical studies such as those by Thirlby [12], McKenzie et al. [4], Tveitereid and Palm [13], and Clever [2] were all based on the assumption that Q is uniform. However, Q is not necessarily uniform in many practical problems with applications in nature or engineering. A non-uniform Q which produces a nonlinear basic temperature gradient may be due to heat release of chemical reactions which take place in the liquid or radioactive decay or ohmic heating by a current in a conductive fluid or heat source produced by radiation from the external medium, and so on. The problem of thermal convection in a horizontal layer of fluid with an internal heat source which is restricted vary linearly with the vertical variable was first studied by Riahi [8]. He has proved that the critical Rayleigh number depends strongly on non-uniform internal heat parameter but weakly depends on internal heat parameter and also showed that the presence of internal heating affect strongly the cell's size, the stability of the convection motion and the internal motion of the hexagonal cells. Pal [7] studied the flow and heat transfer characteristics in unsteady laminar boundary layer of an incompressible viscous fluid over continuously stretching permeable surface in the presence of non-uniform heat source/sink and thermal radiation using Runge-Kutta-Fehlberg method. Siddheshwar and Titus [9] studied linear and non linear Rayleigh-B nard with variable heat source (sink) using Fourier series where the strength of the heat source is characterized by an internal Rayleigh number, and has demonstrated that Ginzburg-Landau model can be derived from the Lorenz model. Mahantesh et al. [1] examined an exponential space-dependent heat source and Marangoni effects on dusty nanofluid boundary layer flow towards a flat surface by utilizing linear/quadratic variation of the surface temperature using Runge-Kutta-Fehlberg method coupled with shooting technique. Sumithra et al. [11] have examined effect of constant heat source/sink and non uniform temperature gradients on Darcian-B nard-Magneto-Marangoni convection in composite layer horizontally enclosed by adiabatic boundaries. A closed form solution is obtained for the thermal Marangoni number. Effects of physical parameters like porous parameter, internal Rayleigh number in both the layers and thermal ration for Marangoni number investigated on linear, parabolic and inverted parabolic temperature profiles. Also, it is observed

that the effect of heat source/sink is dominant in the fluid layer.

This research paper aims at understanding the effect of temperature dependent heat sources on surface tension driven convection in a composite system comprising of an incompressible fluid saturated porous layer over which lies a layer of the same fluid under microgravity condition. This composite layer is bounded below and above by rigid and free boundaries with surface tension effects depending on temperature at free boundary. The eigen value, the thermal Marangoni number is obtained for two sets of temperature boundary combinations set (i) Adiabatic-Adiabatic and set (ii) Adiabatic-Isothermal.

2. Formulation of the Problem

Consider an infinite horizontal layer of a Newtonian fluid of depth ' d ' overlying a fluid saturated isotropic densely packed porous layer of depth ' d_m ' with heat sources Q and Q_m respectively. The lower surface of the porous layer is rigid and the upper surface of the fluid layer is free with the surface tension depending on temperature. A Cartesian coordinate system is chosen with the origin at the interface between porous and fluid layers and the z -axis, vertically upwards. The basic equations governing such a system are,

For the Fluid Layer:

$$\nabla \cdot \vec{q} = 0 \tag{2.1}$$

$$\rho_o \left[\frac{\partial \vec{q}}{\partial t} + (\vec{q} \cdot \nabla) \vec{q} \right] = -\nabla P + \mu \nabla^2 \vec{q} \tag{2.2}$$

$$\frac{\partial T}{\partial t} + (\vec{q} \cdot \nabla) T = \kappa \nabla^2 T + Q(T - T_o) \tag{2.3}$$

For the porous layer:

$$\nabla_m \cdot \vec{q}_m = 0 \tag{2.4}$$

$$\frac{\rho_o}{\phi} \frac{\partial \vec{q}_m}{\partial t_m} = -\nabla_m P_m - \frac{\mu}{K} \vec{q}_m \tag{2.5}$$

$$A \frac{\partial T_m}{\partial t_m} + (\vec{q}_m \cdot \nabla_m) T_m = \kappa_m \nabla_m^2 T_m + Q_m(T_m - T_o) \tag{2.6}$$

where \vec{q} is the velocity vector, ρ_o is the fluid density, t is the time, μ is the fluid viscosity, P is the total pressure, ϕ is the porosity, κ is the thermal diffusivity of the fluid, K is the permeability of the porous medium, $A = \frac{(\rho_o C_p)_m}{(\rho_o C_p)_f}$ is the ratio of heat capacities where C_p is the specific heat, κ_m is the thermal diffusivity of the porous medium, T and T_m denotes temperatures in the fluid and porous medium respectively. Here subscripts m refers to the porous layer and f refers to the fluid layer.

The basic state of fluid and porous layers are assumed to be quiescent, pressure and temperatures are functions of z only. The temperature distributions are found to be

$$T_b(z) = \frac{T_u - T_o}{\sin\left(\sqrt{\frac{Q}{\kappa}d}\right)} \sin\left(\sqrt{\frac{Q}{\kappa}z}\right) + T_o, \quad 0 \leq z \leq d \tag{2.7}$$



$$T_{mb}(z_m) = \frac{T_o - T_L}{\sin\left(\sqrt{\frac{Q_m}{\kappa_m}} d_m\right)} \sin\left(\sqrt{\frac{Q_m}{\kappa_m}} z_m\right) + T_o, \quad -d_m \leq z_m \leq 0 \quad (2.8)$$

where,

$$T_o = \frac{T_u \sqrt{Q\kappa} \sin\left(\sqrt{\frac{Q_m}{\kappa_m}} d_m\right) + T_L \sqrt{Q_m \kappa_m} \sin\left(\sqrt{\frac{Q}{\kappa}} d\right)}{\sqrt{Q_m \kappa_m} \sin\left(\sqrt{\frac{Q}{\kappa}} d\right) + \sqrt{Q\kappa} \sin\left(\sqrt{\frac{Q_m}{\kappa_m}} d_m\right)}$$

is the interface temperature.

Now an infinitesimal perturbations are superimposed in the form

$$\vec{q} = \vec{q}_b + \vec{q}', \quad T = T_b(z) + \theta, \quad P = P_b(z) + P' \quad (2.9)$$

$$\vec{q}_m = \vec{q}_{mb} + \vec{q}_m', \quad T_m = T_{mb}(z_m) + \theta_m, \quad P_m = P_{mb}(z_m) + P_m' \quad (2.10)$$

where the prime indicates a perturbed quantity and the subscript 'b' denotes the basic state. Equations (2.9) and (2.10) are substituted in equations (2.1) to (2.6) and linearized in the usual manner. The pressure term is eliminated from the equations (2.2) and (2.5) by taking curl twice on these two equations and then the resulting equations are non dimensionalized using appropriate scale factors according as Vanishree et al. [14] and Sumithra et al. [11]

The dimensionless equations are subjected to normal mode analysis in the form

$$\begin{bmatrix} W \\ \theta \end{bmatrix} = \begin{bmatrix} W(z) \\ \theta(z) \end{bmatrix} f(x, y) e^{nt} \quad (2.11)$$

$$\begin{bmatrix} W_m \\ \theta_m \end{bmatrix} = \begin{bmatrix} W_m(z_m) \\ \theta_m(z_m) \end{bmatrix} f_m(x_m, y_m) e^{n_m t} \quad (2.12)$$

with $\nabla^2 f + a^2 f = 0$ and $(\nabla_m)^2 f_m + a_m^2 f_m = 0$, where a and a_m are nondimensional horizontal wave numbers, n and n_m are frequencies, $W(z)$ and $W_m(z_m)$ are dimensionless vertical velocities in fluid and porous layers, the following equations are obtained: In $0 \leq z \leq 1$,

$$\left(D^2 - a^2 - \frac{n}{Pr}\right) (D^2 - a^2) W(z) = 0 \quad (2.13)$$

$$(D^2 - a^2 + R_I + n) \theta(z) + W(z) \sqrt{R_I} \frac{\cos(\sqrt{R_I} z)}{\sin \sqrt{R_I}} = 0 \quad (2.14)$$

In $-1 \leq z_m \leq 0$,

$$\left(\frac{n_m \beta^2}{Pr_m} - 1\right) (D_m^2 - a_m^2) W_m(z_m) = 0 \quad (2.15)$$

$$(D_m^2 - a_m^2 - R_{I_m} + n_m A) \theta_m(z_m) + W_m(z_m) \sqrt{R_{I_m}} \frac{\cos(\sqrt{R_{I_m}} z_m)}{\sin \sqrt{R_{I_m}}} = 0 \quad (2.16)$$

where $Pr = \frac{\mu}{\rho_o \kappa}$ is the prandtl number in the fluid layer, $Pr_m = \frac{\phi \mu}{\rho_o \kappa_m}$ is the Prandtl in the porous layer, $\beta^2 = \frac{K}{d_m^2} = Da$ is the darcy number, $R_I = \frac{Q}{\kappa} d^2$ is the internal Rayleigh number for the fluid layer and $R_{I_m} = \frac{Q_m}{\kappa_m} d_m^2$ is the internal Rayleigh number for the porous layer. Obtaining the relevant neutral stability ($n = n_m = 0$), we get, in $0 \leq z \leq 0$,

$$(D^2 - a^2) (D^2 - a^2) W(z) = 0 \quad (2.17)$$

$$(D^2 - a^2 + R_I) \theta(z) + W(z) \sqrt{R_I} \frac{\cos(\sqrt{R_I} z)}{\sin \sqrt{R_I}} = 0. \quad (2.18)$$

In $-1 \leq z_m \leq 0$,

$$(D_m^2 - a_m^2) W_m(z_m) = 0 \quad (2.19)$$

$$(D_m^2 - a_m^2 - R_{I_m}) \theta_m(z_m) + W_m(z_m) \sqrt{R_{I_m}} \frac{\cos(\sqrt{R_{I_m}} z_m)}{\sin \sqrt{R_{I_m}}} = 0 \quad (2.20)$$

Equations (2.17) to (2.20) are decoupled ordinary differential equations. To solve these equations we need six velocity boundary conditions and four temperature boundary conditions.

3. Boundary Conditions

The suitable boundary conditions are non-dimensionalized and then subjected to normal mode analysis. They are:

$$W(1) = 0 \quad (3.1)$$

$$W(0) = \frac{\zeta}{\epsilon_T} W_m(0) \quad (3.2)$$

$$(D^2 + a^2) W(0) = \frac{\zeta^3 \hat{\mu}}{\epsilon_T} (D_m^2 + a_m^2) W_m(0) \quad (3.3)$$

$$(D^3 - 3a^2 D) W(0) = -\frac{\zeta^2 \hat{\mu}}{\epsilon_T Da} D_m W_m(0) \quad (3.4)$$

$$W_m(1-) = 0 \quad (3.5)$$

$$D^2 W(1) + M \theta(1) = 0. \quad (3.6)$$

Here $\hat{\mu} = \frac{\mu_m}{\mu}$ is the viscosity ratio, where μ_m is the effective viscosity of the fluid in the porous layer, and in this paper the value of $\hat{\mu}$ is considered as unity, that is viscosity of the fluid in the fluid layer is same as the viscosity of the fluid in the porous layer, $\zeta = \frac{d}{d_m}$ is the depth ratio, $\epsilon_T = \frac{\kappa}{\kappa_m}$ is the ratio of thermal diffusivity and $M = -\frac{\partial \sigma}{\partial T} \frac{(T_o - T_u) d}{\mu \kappa}$ is the thermal Marangoni number, where σ is the surface tension and T is the temperature.

4. Method of Solution

The velocity equations (2.17) and (2.19) are solved exactly for vertical velocity distributions $W(z)$ and $W_m(z_m)$ and are



suitably obtained as,

$$W(z) = A_1 [\cosh(az) + A_2 \sinh(az) + A_3 z \cosh(az) + A_4 z \sinh(az)] \quad (4.1)$$

$$W_m Z_m = A_1 [A_{m_1} \cosh(a_m z_m) + A_{m_2} \sinh(a_m z_m)] \quad (4.2)$$

where $A_1, A_2, A_3, A_4, A_{m_1}$ and A_{m_2} are constants which are determined by velocity boundary conditions given by equations (3.1), (3.2), (3.3), (3.4) and (3.5) and they are:

$$A_2 = -\frac{\zeta a_m}{2a^3 Da} \coth(a_m), \quad A_3 = -[1 + (A_2 + A_4) \tanh(a)]$$

$$A_4 = \frac{1}{a} [\zeta^2 a_m^2 - a^2], \quad A_{m_1} = \frac{\varepsilon_T}{\zeta}, \quad A_{m_2} = -\frac{\varepsilon_T}{\zeta} \coth(a_m)$$

4.1 Thermal Marangoni number for the set (i) Adiabatic - Adiabatic (A-A) condition

The Adiabatic-Adiabatic temperature boundary conditions on the boundaries of the composite layer are used to solve the temperature distributions $\theta(z)$ and $\theta_m(z_m)$, where both the boundaries of the composite layer are adiabatic. They are as follows:

$$D\theta(1) = 0, \quad \theta(0) = \frac{\varepsilon_T}{\zeta} \theta_m(0), \quad D\theta(0) = D_m \theta_m(0),$$

$$D_m \theta_m(-1) = 0. \quad (4.3)$$

The temperature distributions obtained by solving equations (2.18) and (2.20) using velocity distributions (4.1) and (4.2) are,

$$\theta(z) = A_1 [c_1 \cosh(bz) + c_2 \sinh(bz) - f(z)] \quad (4.4)$$

$$\theta_m(z_m) = A_1 [c_3 \cosh(b_m z_m) + c_4 \sinh(b_m z_m) - f_m(z_m)] \quad (4.5)$$

where $b = \sqrt{a^2 - R_I}$ and $b_m = \sqrt{a_m^2 - R_{I_m}}$. The coefficients c_1, c_2, c_3 and c_4 are obtained by using temperature boundary conditions (4.3) and are as follows:

$$c_1 = \delta_1 + \frac{\varepsilon_T}{\zeta} c_3, \quad c_2 = \frac{\delta_3 - c_1 b \sinh(b)}{b \cosh(b)}, \quad c_4 = \frac{c_3 b_m \sinh(b_m)}{b_m \cosh(b_m)}$$

$$c_3 = \frac{-b\delta_1 \sinh(b) \cosh(b_m) - \delta_2 \cosh(b) \cosh(b_m) + \delta_3 \cosh(b_m) + \delta_4 \cosh(b)}{b_m \sinh(b_m) \cosh(b) + \frac{\varepsilon_T}{\zeta} b \sinh(b) \cosh(b_m)}$$

$$\delta_1 = \left(\frac{A_4}{2a\sqrt{R_I} \sin(\sqrt{R_I})} \right),$$

$$\delta_2 = \left(\frac{\sqrt{R_I}}{2a \sin(\sqrt{R_I})} \right) \left(A_2 - \frac{A_3}{a} + \frac{aA_3}{R_I} \right) - \left(\frac{A_{m_2} \sqrt{R_{I_m}}}{2a_m \sin(\sqrt{R_{I_m}})} \right)$$

$$\delta_3 = \frac{1}{2a \sin(\sqrt{R_I})} (\Lambda_1 + A_2 \Lambda_2 + A_3 \Lambda_3 + A_4 \Lambda_4)$$

$$\Lambda_1 = a \cosh(a) \sin(\sqrt{R_I}) + \sqrt{R_I} \sinh(a) \cos(\sqrt{R_I})$$

$$\Lambda_2 = a \sinh(a) \sin(\sqrt{R_I}) + \sqrt{R_I} \cosh(a) \cos(\sqrt{R_I})$$

$$\Lambda_3 = a \sin(\sqrt{R_I}) \cosh(a) + \sqrt{R_I} \cosh(a) \cos(\sqrt{R_I})$$

$$- \frac{1}{a} \sqrt{R_I} \cos(\sqrt{R_I}) \cosh(a)$$

$$- \sin(\sqrt{R_I}) \sinh(a) + \frac{a}{\sqrt{R_I}} \cos(\sqrt{R_I}) \cosh(a)$$

$$\Lambda_4 = \Lambda_{41} + \Lambda_{42}$$

$$\Lambda_{41} = a \sin(\sqrt{R_I}) \sinh(a) + \sqrt{R_I} \cos(\sqrt{R_I}) \cosh(a)$$

$$- \sin(\sqrt{R_I}) \cosh(a)$$

$$\Lambda_{42} = \left(\frac{a}{\sqrt{R_I}} - \frac{\sqrt{R_I}}{a} \right) \cos(\sqrt{R_I}) \sinh(a)$$

$$\delta_4 = \frac{1}{2a_m \sin(\sqrt{R_{I_m}})} (A_{m_1} \lambda_1 - A_{m_2} \lambda_2)$$

$$\lambda_1 = a_m \cosh(a_m) \sin(\sqrt{R_{I_m}}) + \sqrt{R_{I_m}} \sinh(a_m) \cos(\sqrt{R_{I_m}})$$

$$\lambda_2 = a_m \sinh(a_m) \sin(\sqrt{R_{I_m}}) + \sqrt{R_{I_m}} \cos(\sqrt{R_{I_m}}) \cosh(a_m).$$

The eigen value thermal Marangoni number M obtained from the boundary condition (3.6) is:

$$M = -\frac{D^2 W(1)}{a^2 \theta(1)}$$

and using the same condition for the set (i) Adiabatic-Adiabatic condition, the thermal Marangoni number is:

$$M_{AA} = -\frac{m_{11} \cosh(a) + m_{12} \sinh(a)}{a^2 \left(m_{21} - \left(\frac{1}{2a \sin(\sqrt{R_I})} \right) (m_{22} + A_3 m_{23} + A_4 m_{24}) \right)} \quad (4.6)$$

$$m_{11} = a^2 (1 + A_3) + 2aA_4, \quad m_{12} = a^2 (A_2 + A_3) + 2aA_3$$

$$m_{21} = c_1 \cosh(b) + c_2 \sinh(b)$$

$$m_{22} = \sinh(a) \sin(\sqrt{R_I}) + A_2 \cosh(a) \sin(\sqrt{R_I})$$

$$m_{23} = \sinh(a) \sin(\sqrt{R_I}) - \frac{1}{a} \sin(\sqrt{R_I}) \cosh(a)$$

$$+ \frac{1}{\sqrt{R_I}} \cos(\sqrt{R_I}) \sinh(a)$$

$$m_{24} = \sin(\sqrt{R_I}) \cosh(a) - \frac{1}{a} \sin(\sqrt{R_I}) \sinh(a)$$

$$+ \frac{1}{\sqrt{R_I}} \cos(\sqrt{R_I}) \cosh(a)$$

4.2 Thermal Marangoni number for the set (i) Adiabatic - Isothermal (A-I) condition

The Adiabatic-Isothermal temperature boundary conditions on the boundaries of the composite layer are used to solve the temperature distributions $\theta(z)$ and $\theta_m(z_m)$, where the upper boundary of the fluid layer is adiabatic and the lower boundary of the porous layer is isothermal and they are as follows:

$$D\theta(1) = 0, \quad \theta(0) = \frac{\varepsilon_T}{\zeta} \theta_m(0), \quad D\theta(0) = D_m \theta_m(0),$$

$$\theta_m(-1) = 0 \quad (4.7)$$



The temperature distributions are obtained by solving equations (2.18) and (2.20) using the velocity distributions (4.1) and (4.2) and are as follows:

$$\theta(z) = A_1 [c_{11} \cosh(bz) + c_{12} \sinh(bz) - f(z)] \quad (4.8)$$

$$\theta_m(z_m) = A_1 [c_{23} \cosh(b_m z_m) + c_{24} \sinh(b_m z_m) - f_m(z_m)] \quad (4.9)$$

The coefficients c_{11} , c_{12} , c_{23} and c_{24} are obtained by using temperature boundary conditions (4.7) and are as follows:

$$c_{11} = \delta_1 + \frac{\epsilon_T}{\zeta} c_{23}, \quad c_{12} = \frac{\delta_{12} + c_{24} b_m}{b}, \quad c_{23} = \frac{\Delta_1 + \Delta_2}{\Delta_{12}},$$

$$c_{24} = \frac{c_{23} \cosh(b_m) - \delta_{mII}}{\sinh(b_m)},$$

$$\Delta_1 = -b\delta_1 \sinh(b) \sinh(b_m) - \delta_2 \cosh(b) \sinh(b_m)$$

$$\Delta_2 = \delta_{mII} b_m \cosh(b) + \delta_3 \sinh(b_m),$$

$$\Delta_{12} = b_m \cosh(b_m) \cosh(b) + \frac{\epsilon_T}{\zeta} b \sinh(b) \sinh(b_m)$$

$$\delta_{mII} = \frac{1}{2a_m \sin(\sqrt{R_{Im}})} (A_{m1} \Delta_3 - A_{m2} \Delta_4)$$

$$\Delta_3 = a_m \cosh(a_m) \sin(\sqrt{R_{Im}}) + \sqrt{R_{Im}} \sinh(a_m) \cos(\sqrt{R_{Im}})$$

$$\Delta_4 = a_m \sinh(a_m) \sin(\sqrt{R_{Im}}) + \sqrt{R_{Im}} \cosh(a_m) \cos(\sqrt{R_{Im}})$$

The eigen value, thermal Marangoni number obtained from boundary condition (3.6) is:

$$M = -\frac{D^2 W(1)}{a^2 \theta(1)}$$

and using the same condition for the set (ii) Adiabatic-Isothermal condition, the thermal Marangoni number is:

$$M_{AI} = -\frac{m_{11} \cosh(a) + m_{12} \sinh(a)}{a^2 \left(m_{21} - \left(\frac{1}{2a \sin(\sqrt{R_I})} \right) (m_{22} + A_3 m_{23} + A_4 m_{24}) \right)} \quad (4.10)$$

$$m_{11} = a^2 (1 + A_3) + 2aA_4, \quad m_{12} = a^2 (A_2 + A_3) + 2aA_3$$

$$m_{21} = c_1 \cosh(b) + c_2 \sinh(b)$$

$$m_{22} = \sinh(a) \sin(\sqrt{R_I}) + A_2 \cosh(a) \sin(\sqrt{R_I})$$

$$m_{23} = \sinh(a) \sin(\sqrt{R_I}) - \frac{1}{a} \sin(\sqrt{R_I}) \cosh(a) + \frac{1}{\sqrt{R_I}} \cos(\sqrt{R_I}) \sinh(a)$$

$$m_{24} = \sin(\sqrt{R_I}) \cosh(a) - \frac{1}{a} \sin(\sqrt{R_I}) \sinh(a) + \frac{1}{\sqrt{R_I}} \cos(\sqrt{R_I}) \cosh(a)$$

5. Result and Discussion

The effect of surface tension driven convection in a composite system consisting of a fluid layer saturated by the same system is investigated theoretically.

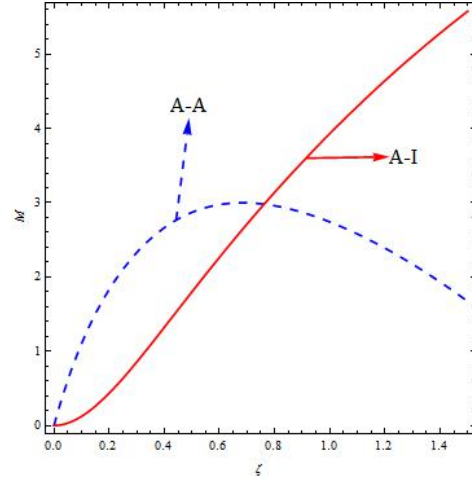


Figure 1. Comparison of thermal Marangoni number for A-A and A-I

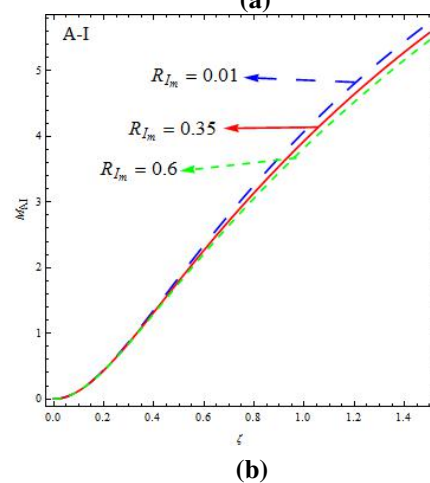
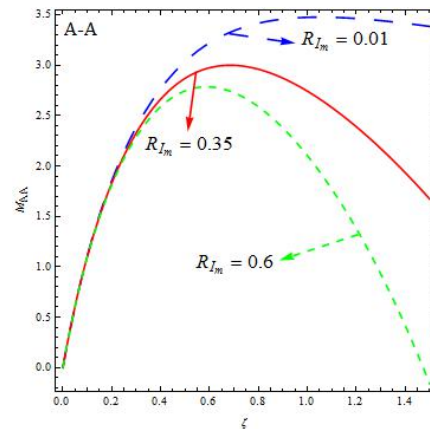


Figure 2. Effects of internal Rayleigh number R_{Im}

The eigen value problem is solved exactly and an analytical expression for the thermal Marangoni number is obtained for two types of temperature boundary conditions, viz., (i) both the boundaries of the composite layer are adiabatic(A-A), (ii) lower rigid boundary is isothermal and upper free surface is



adiabatic(A-I). The effects of R_I , R_{I_m} , the internal Rayleigh

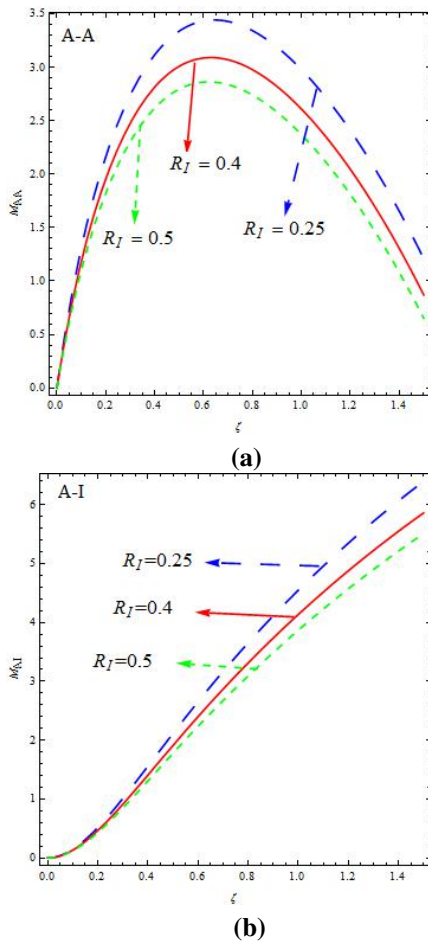


Figure 3. Effects of internal Rayleigh number R_I

numbers for the fluid and porous layers, the horizontal wave number a , the thermal diffusivity ratio ϵ_T , and the Darcy number Da on the Marangoni number are displayed in the following figures where the supplementary parameters are fixed.

The comparison of thermal Marangoni numbers as a function of depth ratio ζ for the Adiabatic-Adiabtic(A-A) and Adiabatic-Isothermal(A-I)temperature boundary conditions is shown in Figure 1. It is observed that in case of A-A boundaries, the thermal Marangoni number M_{AA} increases initially with ζ and reaches maximum and then decreases with further increase in ζ . In case of A-I boundaries, thermal marangoni number M_{AI} increases with increase in ζ without any decreasing trend as noticed in case of A-A boundaries. For smaller values of depth ratio, the system is stable when A-A temperature boundary conditions are deployed, whereas for larger values of depth ratio the same system is stable for A-I temperature boundary combinations. But both M_{AA} and M_{AI} coincide when the value of the depth ratio is $\zeta = \frac{d}{d_m} = 0.75$.

Figures (2a) and (2b) are the plots of M_{AA} and M_{AI} versus the depth ratio ζ for the linear temperature distribution for

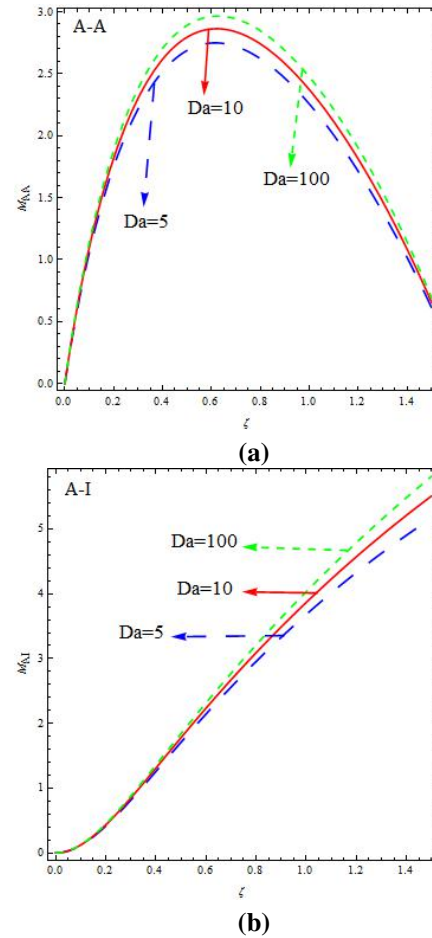


Figure 4. Effects of Darcy number Da

different porous internal Rayleigh number R_{I_m} when the other parameters are fixed. In case of A-A boundaries, it is observed that M_{AA} increases initially with ζ and reaches maximum and then decreases with further increase in ζ . One important observation that can be made from fig (2a) is that when the strength of the heat source is small ($R_{I_m} = 0.01$), M_{AA} attains maximum with increasing ζ up to a certain epth ratio and then remains the same with further increase in ζ , whereas for $R_{I_m} = 0.35$ and 0.6 , M_{AA} increase with ζ , attains maximum and decreases with further increase in ζ . This indicates that the choice of the strength of heat source plays a crucial role in the stability of the system. It is also observed that increase in R_{I_m} decreases M_{AA} and thus destabilizes the system. this indicates that the increase in the strength of the heat source in the porous layer decreases the surface tension thereby decreasing M_{AA} . From Fig. 2b we notice that the thermal Marangoni number M_{AI} increases with increase in ζ and decreases with increase in R_{I_m} for the A-I boundaries and thus destabilize the system. one can see from these graphs that the effect of R_{I_m} is more dominant in the case of A-A temperature boundary conditions. It is also observed that for different R_{I_m} , both M_{AA} and M_{AI} remain same till ζ attains a certain value. This implies that the effect of R_{I_m} is significant in the porous dominant composite



layer.

Thermal Marangoni numbers M_{AA} and M_{AI} as a function of

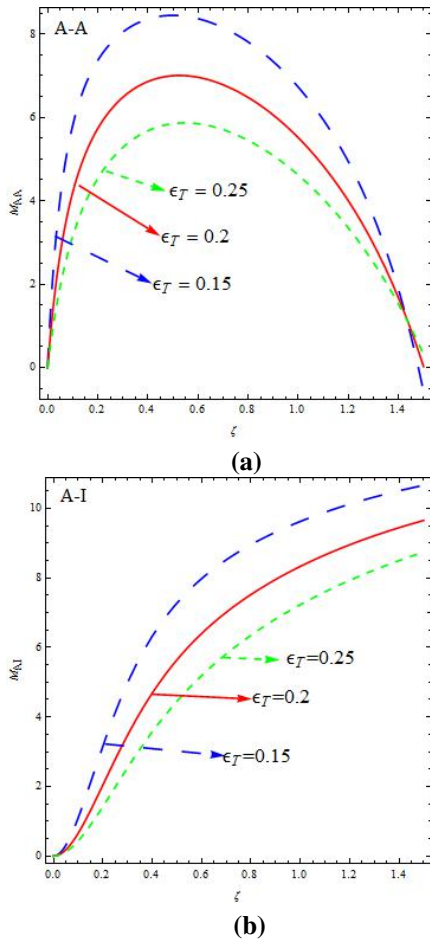


Figure 5. Effects of thermal diffusivity ratio ϵ_T

depth ratio ζ for linear temperature distribution are shown in Figs. 3a and 3b. The effect of fluid internal Rayleigh number, R_I for a set of fixed physical parameters $a = 1, R_{Im} = \epsilon_T = 0.5, Da = 10$ and different values of $R_I = 0.25, 0.4, 0.5$. In case of A-A boundary combination (Fig. 3a), it is observed that M_{AA} increases initially with ζ and reaches maximum and then decreases with further increase in ζ . In case of A-I boundary combination (Fig. 3b), M_{AI} increases with increase in ζ without any decreasing trend as noticed in case of A-A boundaries. Also, it is observed that M_{AA} and M_{AI} decrease with increase in R_I for both the cases and thus destabilize the system. All other observations are qualitatively similar to those observed in Figs. 2a and 2b.

The variations in M_{AA} and M_{AI} as a function of ζ in Figs. 4a and 4b, respectively for $Da = 5, 10, 100$ when $R_I = R_{Im} = \epsilon_T = 0.5$ and $a = 1$. In case of A-A boundaries (Fig. 4a), it is seen that M_{AA} increases initially with ζ and reaches maximum and then decreases with further increase in ζ . It is also observed that increase in Da is to increase the thermal Marangoni number M_{AA} and thus stabilize the system. This result is in tune with the intuition, physically Da increase implies

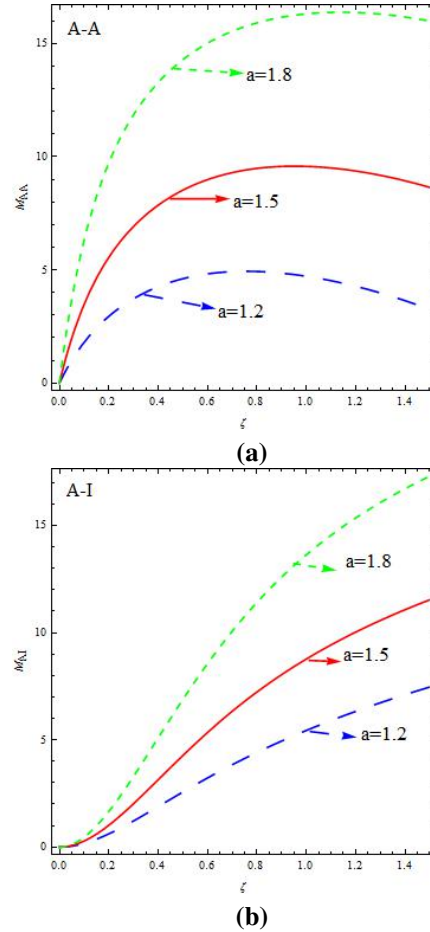


Figure 6. Effects of wave number a

the increase in the permeability there by allowing the flow of more fluid which delays the onset of convection. In case of A-I boundaries (Fig. 4b) also M_{AI} increases with increase in ζ as well as Da and thus stabilize the system.

The effect of thermal diffusivity ratio ϵ_T as a function of ζ for a set of fixed physical parameters $R_I = R_{Im} = 0.5, a = 1, Da = 10$ and different values of $\epsilon_T = 0.15, 0.2, 0.25$ in case of A-A and A-I boundaries are depicted in Figs. 5a and 5b. From Fig. 5a, it is seen that M_{AA} increases initially with ζ reaches maximum and then decreases with further increase in ζ , whereas in case of A-I boundaries, M_{AI} increases with increase in ζ as shown in Fig. 5b. Also it is observed that increase in ϵ_T decreases M_{AA} and M_{AI} in both the cases and thus having a destabilizing effect on the system. Physically, increase in thermal diffusivity increases the heat transfer rate which destabilizes the system.

Figures 6a and 6b show variations in M_{AA} and M_{AI} with ζ for different values of horizontal wave number $a = 1.2, 1.5, 1.8$ when $R_I = R_{Im} = \epsilon_T = 0.5$ and $Da = 10$. In case of A-A and A-I boundaries, we observe that an increase in ζ increases M_{AA} and M_{AI} respectively. This is because increase in depth ratio decreases the temperature at the surface thereby increasing the surface tension due to the increase in cohesive force



with decrease in molecular thermal activity. Also increase in wave number 'a' increases thermal Marangoni numbers M_{AA} and M_{AI} thus stabilizing system. Physically increase in wave number, decreases the cell size and hence increase the thermal Marangoni numbers M_{AA} and M_{AI} .

6. Conclusion

The effect of temperature dependent heat source on surface tension driven convection in a composite system comprising of an incompressible fluid saturated porous layer over which lies a layer of the same fluid is analyzed theoretically. The following conclusions are drawn from the above results.

1. The effect of internal Rayleigh numbers, both R_{Im} and R_I , and thermal diffusivity ratio ε_T is to destabilize the system and that of porous parameter Da and the wave number a is to stabilize the system for both the boundaries viz., A-A and A-I.
2. The strength of heat source in both porous and fluid layer, R_{Im} and R_I , can be effectively chosen to control the convection.
3. $M_{AA}(\zeta) < M_{AI}(\zeta)$ for all parameters except for smaller depth ratios.

References

- [1] Basavarajappa Mahanthesh, Bijjanal Jayanna Gireesha, Ballajja Chandra PrasannaKumara, Nagavangala Shankarappa Shashikumar, Marangoni convection radiative flow of dusty nanoliquid with exponential space dependent heat source, *Nuclear Engineering and Technology*, 49(8)2017, 1660-1668.
- [2] R. M. Clever, Heat transfer and stability properties of convection rolls in an internally heated fluid layer, *Journal of Applied Mathematics and Physics (ZAMP)* 28(1977), 585-597.
- [3] Y. H. Gangadharaiah, Onset of Benard-Marangoni convection in a composite layer with anisotropic porous material, *Journal of Applied Fluid Mechanics*, 9(3)(2016), 1551-1558.
- [4] D. McKenzie, J. Roberts and N. Weiss, Convection in the earth's mantle: Towards a numerical simulation, *Journal of Fluid Mechanics*, 62(3)(1974), 465-538.
- [5] D. A. Nield, Onset of convection in a fluid layer overlying a layer of porous medium, *Journal of Fluid Mechanics*, 81(1977), 513-522.
- [6] D. A. Nield, Modelling the effect of surface tension on the onset of natural convection in a saturated porous medium, *Transport Porous Med*, 31(1988), 365-368.
- [7] D. Pal, Combined effects of non-uniform heat source/sink and thermal radiation on heat transfer over an unsteady stretching permeable surface, *Commun. Non-linear Sci. Numer. Simulat*, 16(2011), 1890-1904.
- [8] N. Riahi, Nonlinear Convection in a Horizontal Layer with an Internal Heat Source, *J.Phys. Soc. Jpn*, 53(1984), 4169-4178.
- [9] P. G. Siddheshwar and P. Stephen Titus, Nonlinear Rayleigh-Bénard Convection with Variable Heat Source, *ASME. J. Heat Transfer*, 135(12)(2013), 122502.
- [10] I. S. Shivakumara, S. P. Suma, R. Indira, Effect of Internal Heat Generation on the Onset of Marangoni Convection in a Fluid Layer Overlying a Layer of an Anisotropic Porous Medium, *Transp Porous Med*, 92(2012), 727-743.
- [11] R. Sumithra and N. Manjunath, Effects of heat source/sink and non uniform temperature gradients on Darcian-Bénard-Magneto-Marangoni convection in a composite layer horizontally enclosed by adiabatic boundaries, *Malaya Journal of Matematik*, 8(2)(2020), 373-382.
- [12] R. Thirlby, Convection in an Internally Heated Layer, *J. Fluid Mech*, 44(1970), 673-693.
- [13] M. Tveitereid and E. Palm, Convection Due to Internal Heat Sources, *J. Fluid Mech*, 76(3)(1976), 481-499.
- [14] R. K. Vanishree, R. Sumithra and N. Manjunatha, Effect of uniform and non-uniform temperature gradients on Benard-Marangoni convection in a superposed fluid and porous layer in the presence of heat source, *Gedrag and Organisatie Review*, 33(2)(2020), 746-758.

ISSN(P):2319 – 3786

Malaya Journal of Matematik

ISSN(O):2321 – 5666

